communications biology

Article

https://doi.org/10.1038/s42003-024-07225-y

Phosphatidic acid directly activates mTOR and then regulates SREBP to promote ganoderic acid biosynthesis under heat stress in *Ganoderma lingzhi*

Yong-Nan Liu[1,2] ✉, Yu-Lin Chen[1,2], Zi-Juan Zhang[1,2], Feng-Yuan Wu[1,2], Hao-Jin Wang[1,2], Xiao-Ling Wang[1,2] & Gao-Qiang Liu[1,2] ✉

Ganoderic acids (GAs), a class of secondary metabolites produced by the traditional medicinal mushroom *Ganoderma*, are a group of triterpenoids with superior biological activities. Heat stress (HS) is one of the most important environmental abiotic stresses. Understanding how organisms sense temperature and integrate this information into their metabolism is important for determining how organisms adapt to climate change and for applying this knowledge to breeding. We previously reported that HS induced GA biosynthesis, and phospholipase D (PLD)-mediated phosphatidic acid (PA) was involved in HS-induced GA biosynthesis. We screened a proteome to identify the PA-binding proteins in *G. lingzhi*. We reported that PA directly interacted with mTOR and positively correlated with the ability of mTOR to promote GA biosynthesis under HS. The PA-activated mTOR pathway promoted the processing of the transcription factor sterol regulatory element-binding protein (SREBP) under HS, which directly activated GA biosynthesis. Our results suggest that SREBP is an intermediate of the PLD-mediated PA-interacting protein mTOR in HS-induced GA biosynthesis. Our report established the link between PLD-mediated PA production and the activation of mTOR and SREBP in the HS response and HS-induced secondary metabolism in filamentous fungi.

Fungi are extraordinary organisms that readily produce a diverse set of natural products called secondary metabolites, some of which are beneficial to humankind[1]. *Ganoderma*, named "Lingzhi" in Chinese or "Reishi" in Japanese, is widely recognized as a medicinal basidiomycete. *Ganoderma lingzhi* (formerly mistaken for *G. lucidum*) is a species distributed in East Asia and a prize medicinal mushroom that has been recorded in the Chinese Pharmacopoeia and American Herbal Pharmacopoeia and Therapeutic Compendium because of its secondary metabolites, especially ganoderic acids (GAs) (oxygenated lanostane-type triterpenoids), which have multiple pharmacological activities[2,3]. Modern pharmacological and clinical studies have demonstrated that several individual GAs have anti-tumour effects[4,5], liver-protective effects[6], antiviral effects[7,8], and anti-atherosclerotic effects[9] and may be used as treatments for neurological disorders[10,11]. Therefore, the production of GA from *Ganoderma* by modern fermentation has good application prospects. Progress has been made in enhancing GA production in *Ganoderma* species via the manipulation of fermentation strategies[12,13], the addition of chemical inducers[14,15] and genetic engineering[16,17].

In addition to studies on enhancing the production of GA in *Ganoderma*, some work has been conducted to study the regulatory mechanism of GA biosynthesis. To date, the roles of reactive oxygen species[18], Ca^{2+} [19], cAMP[20] and phospholipid signalling[21,22] in GA biosynthesis have been preliminarily elucidated. However, the downstream pathways (loci/target) of these known signalling molecules in the regulation of GA biosynthesis are poorly understood. We previously reported that phospholipase D (PLD)-mediated phosphatidic acid (PA) was involved in GA biosynthesis under heat stress (HS)[21]. However, the molecular mechanism of PA regulation of GA biosynthesis has not been elucidated.

PA is the simplest glycerophospholipid naturally occurring in living organisms and a minor component of membranes, and it has received increasing interest due to its potential for multiple biological functions. For

[1]Hunan Provincial Key Laboratory of Forestry Biotechnology and International Cooperation Base of Science and Technology Innovation on Forest Resource Biotechnology, Central South University of Forestry and Technology, Changsha, China. [2]Laboratory of Yuelushan Seed Industry, Changsha, China. ✉e-mail: ynliu@csuft.edu.cn; gaoliuedu@csuft.edu.cn

example, as a key intermediate metabolite in the synthesis of all membrane glycerophospholipids, PA contributes to membrane biogenesis and plays an important structural role in living cells[23]. PA is also an essential signalling molecule involved in diverse cellular functions in animals, such as cell proliferation and cytoskeletal rearrangement, via the recruitment of a range of cytosolic effector proteins to appropriate membrane locations[24]. In addition, PA binds directly to and activates mammalian target of rapamycin (mTOR, a member of the phosphoinositide 3-kinase-like protein kinase family) in HEK293 cells[25]. Enhanced production of PA by the over-expression of PLD also results in aberrant mTOR activation in mammalian cells[26]. In plants, PAs are recognized as a class of signalling messengers that bind to various proteins, including transcription factors, protein kinases, lipid kinases, and protein phosphatases, and are involved in various plant processes[27]. For example, PLD-mediated PAs interact with constitutive triple response 1, which functions as a negative regulator of the ethylene signalling pathway in response to hypoxia in Arabidopsis[28,29]. PA interacts with a myeloblastosis transcription factor and modulates its nuclear translocation and root hair cell differentiation in Arabidopsis[30]. PA also interacts with and modulates the function of the core clock regulators late elongated hypocotyl and circadian clock associated 1 to regulate the circadian clock in Arabidopsis[31]. However, there are few studies on the biological regulatory function of PA in microorganisms, and little is known about PA-interacting proteins.

In this study, we screened a proteome to identify potential PA-binding proteins in *G. lingzhi*. We report that PA directly interacts with mTOR and is positively correlated with the ability of mTOR to promote GA biosynthesis under HS. In addition, PA-induced activation of the mTOR pathway promotes the processing and activity of the transcription factor

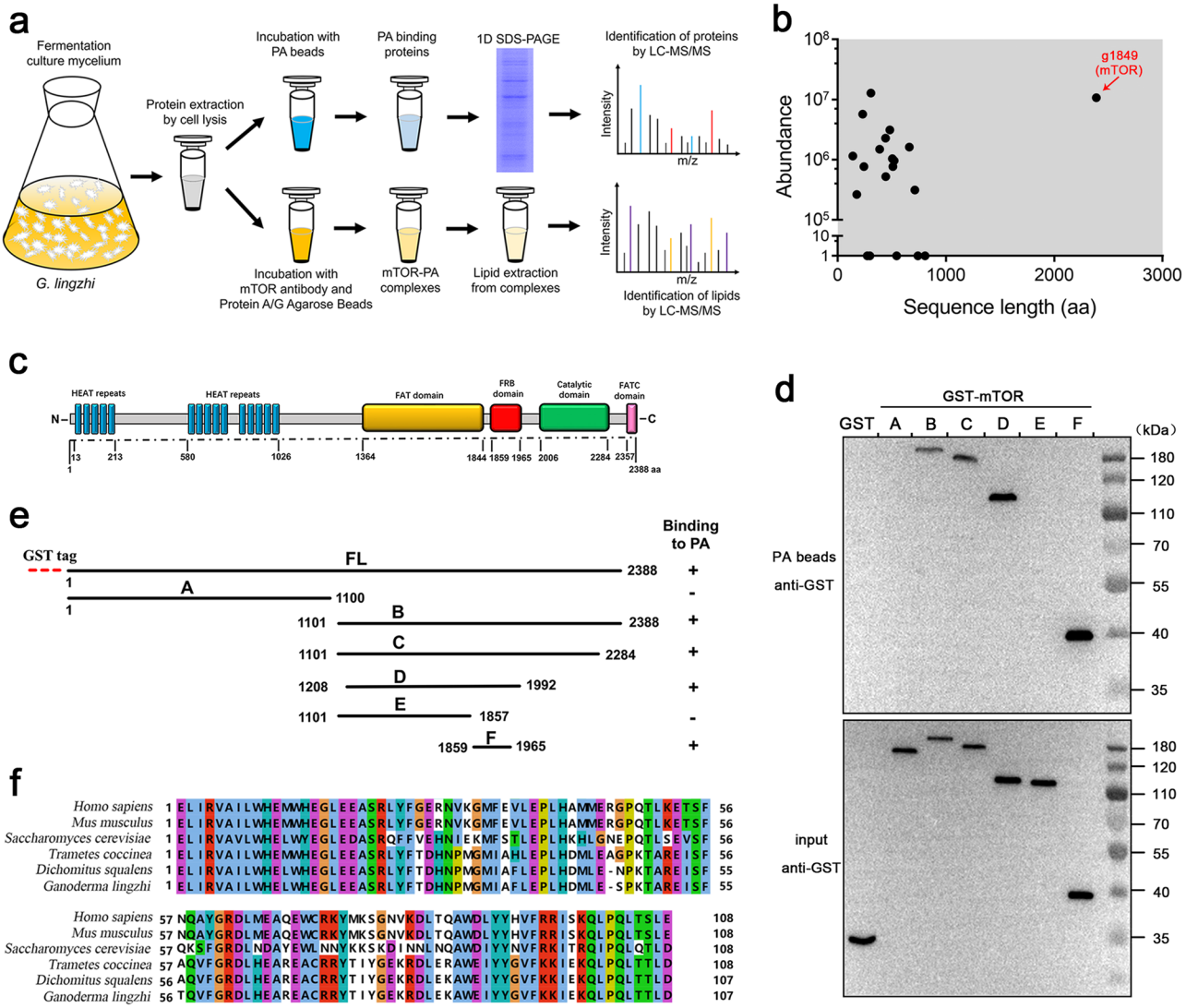

Fig. 1 | Identification and analysis of PA binding mTOR. a Screening of PA binding proteins in vitro and test mTOR interacting with PA in vivo. Experimental setup: cell lysates of 5-d-old mycelia were incubated with PA beads. The bound proteins were subsequently eluted, separated by SDS-PAGE, and analyzed by liquid chromatography coupled to high-resolution tandem mass spectrum (LC-MS/MS). An aliquot of the cell lysates were used to isolate the PA-mTOR complex by using an anti-mTOR antibody to immunoprecipitate mTOR. The bound lipids were extracted and analyzed by LC-MS/MS. **b** Scatter plot of abundance-versus-sequence length of identified PA binding proteins. Arrows mark examples of PA binding mTOR. **c** Features of mTOR protein in *G. lingzhi*. Conserve domain analysis of *G. lingzhi* mTOR was calculated online by NCBI Conserved Domains Database. **d** Characterization of the PA binding domain of mTOR. Pulldown of GST or the recombinant, GST-tagged, indicated regions of mTOR interaction with the PA beads (Top panel). An aliquot of the protein samples (starting material, input) added to the PA beads was analysed in parallel (bottom panel). PA-binding was detected by immunoblotting using a GST-specific antibody. **e** Schematic of serial deletions of the GST-fusion proteins of the mTOR used in (**d**) and the relative strength of binding to PA. FL, full-length mTOR (amino acids 1 to 2388); A, amino acids 1 to 1100; B, amino acids 1101 to 2388; C, amino acids 1101 to 2284; D, amino acids 1208 to 1992; E, amino acids 1101 to 1857; F, amino acids 1859 to 1965. **f** The FRB sequences alignment were performed using clustal omega. Accession numbers for the aligned proteins were indicated in Supplementary Fig. 1.

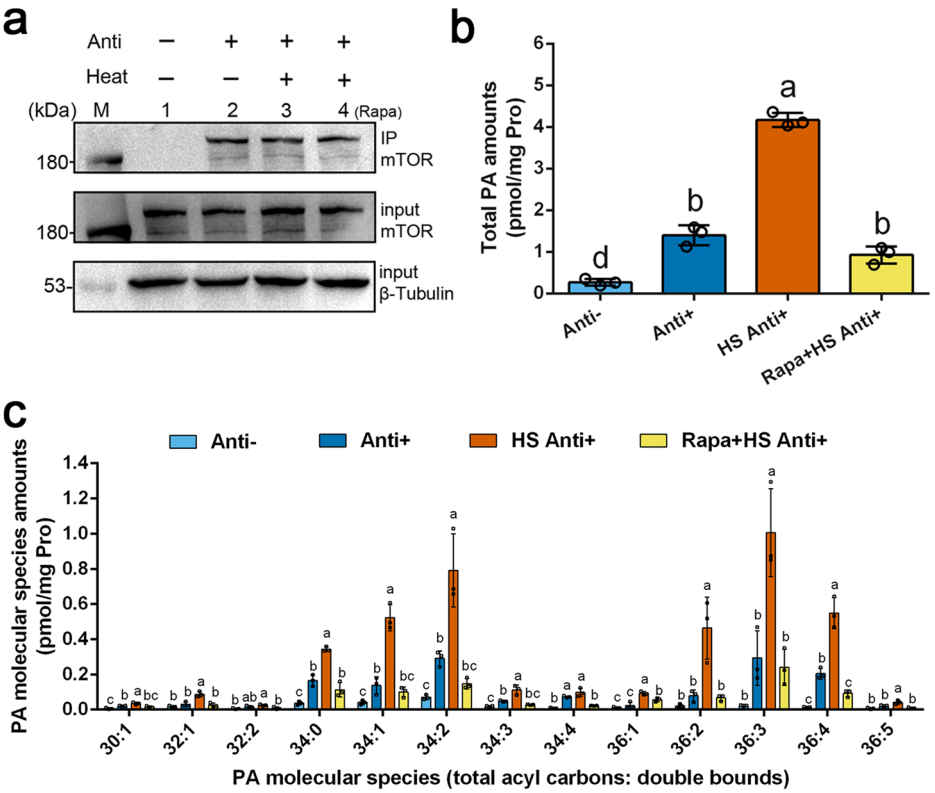

Fig. 2 | Mass spectrometric confirmation of PA-mTOR binding in vivo. a Isolation of mTOR by immunoprecipitation. mTOR was immunoprecipitated using an anti-mTOR antibody from cell lysates of mycelia, and was probed by immunoblotting using the same antibody. + and - indicate with and without antibody (lines 1 and 2), with and without HS for 30 min (lines 2 and 3), respectively, in the immunoprecipitation. Line 4 indicated mycelia were pre-incubation with 100 nM rapamycin for 30 min before being exposed to HS in the immunoprecipitation. Middle and bottom blot shows protein input (mTOR and β-Tubulin) used for the immunoprecipitation. **b** Coprecipitation of total PA with mTOR. Total PA extracted from mTOR immunoprecipitated in **a** was quantified by ESI-MS/MS. **c** Coprecipitation of PA species with mTOR. PA species from total PA extracted in (**b**). The values in (**b**) and (**c**) are the means ± SD ($n = 3$ independent experiments). Different letters in (**b**) and (**c**) indicate significant differences between the lines in the total PA and same PA species, respectively ($P < 0.05$, according to Duncan's multiple range test).

sterol regulatory element-binding protein (SREBP) under HS, which directly activated GA biosynthesis in our previous study[32]. Our results revealed that SREBP was an intermediate of the PLD-mediated PA-interacting protein mTOR in HS-induced GA biosynthesis in *G. lingzhi*.

Results

Identification of PA-interacting mTOR in vitro

To investigate the mechanism of action of PA in GA biosynthesis, we screened the *G. lingzhi* proteome to identify the PA-binding proteins using the pull down assay with PA-conjugated beads (Fig. 1a). Our experiments identified 20 potential PA-interacting proteins. A phosphatidylinositol kinase–like protein kinase (g1849) was one of the proteins specifically coprecipitated with PA and was identified by mass spectrometry to contain 2388 amino acids with a deduced protein molecular weight of 270.8 kDa (Fig. 1b; Supplementary Data 1 and 2).

Conserved domain analysis revealed that g1849 was characterized by a FAT-carboxy terminal domain (FAT domain), a FRAP-ATM-TTRAP domain (FATC domain), a FKBP12-rapamycin binding domain (FRB domain), a kinase catalytic domain, a catalytic domain with kinase activity and two Huntingtin-Elongation factor 3-regulatory subunit A domains of the PP2A-TOR1 repeats (HEAT repeats) (Fig. 1c). Evolutionary relationship analysis revealed that g1849 shared high identity with the other mTOR genes of basidiomycetes. *G. lingzhi* g1849 exhibited 91% identity with *Dichomitus squalens* mTOR, and g1849 was separated from the mTOR of ascomycetes, plants and animals (Supplementary Fig. 1). Taken together, these results indicated that g1849 was a protein kinase mechanistic target of rapamycin (mTOR).

Binding to PA is mediated via the FRB domain of *G. lingzhi* mTOR

To validate and test the specificity domain of the PA interaction, we produced serial deletions of the GST fusion proteins of *G. lingzhi* mTOR from *E. coli* and pulled down each of the six mTOR regions (A, B, C, D, E, and F) using PA-conjugated beads. Deletion of the amino acid residue a.a.1–1100 (A region) of the N-terminus did not affect the PA binding of mTOR, but deletion of a.a.1101–2388 (B region) of the C-terminus abolished PA binding to mTOR (Fig. 1d, e), which indicated that the PA binding region resided in the C-terminal 1101–2388 amino acid residues. Deletion of a.a.2285–2388 and a.a.1993–2388 of the B region did not affect PA binding to mTOR, but deletion of a.a.1858–2388 of the B region abolished PA binding to mTOR. In addition, the peptide consisting of only the a.a.1859-1965 (F region) of the B region exhibited PA binding (Fig. 1d, e). Taken together, domain mapping showed that the FRB domain of mTOR was responsible for the interaction of *G. lingzhi* with PA. We also performed a conservative analysis of the FRB domain based on multiple sequence alignment (Fig. 1f) and showed that the FRB of *G. lingzhi* was conserved in comparison with other known FRB in *Homo sapiens*, *Mus musculus* and several fungi (*Saccharomyces cerevisiae*, *Dichomitus squalens* and *Trametes coccinea*).

Confirmation of binding via isolation of PA-mTOR complexes from *G. lingzhi*

To test whether mTOR interacted with PA in vivo, we isolated the PA-mTOR complex using an anti-mTOR antibody to immunoprecipitate mTOR from *G. lingzhi* mycelia and analysed lipids that coprecipitated with mTOR using mass spectrometry (Fig. 1a). The successful isolation of mTOR was confirmed by immunoblotting, which detected the mTOR band in the precipitates from *G. lingzhi* mycelia with the antibody (Anti+) but not in those without the mTOR antibody (Anti-; Fig. 2a). A significant amount of PA was detected in the sample immunoprecipitated from the Anti+ group compared to the negative control group (Anti-; Fig. 2b). Further analysis of the molecular species of PA revealed that 16C- and 18C-containing PA species, such as 34:0-PA, 34:1-PA, 34:2-PA, 36:2-PA, 36:3-PA, and 36:4-PA, were precipitated with mTOR (Fig. 2c).

These results described above suggest that mTOR interacts with PA in vitro and in vivo. Our previous studies revealed that HS induced a significant accumulation of PA[21]. Therefore, we explored the interaction between PA and mTOR under HS conditions using immunoprecipitation. After treatment with HS for 30 min, the PA-mTOR complex was isolated using an

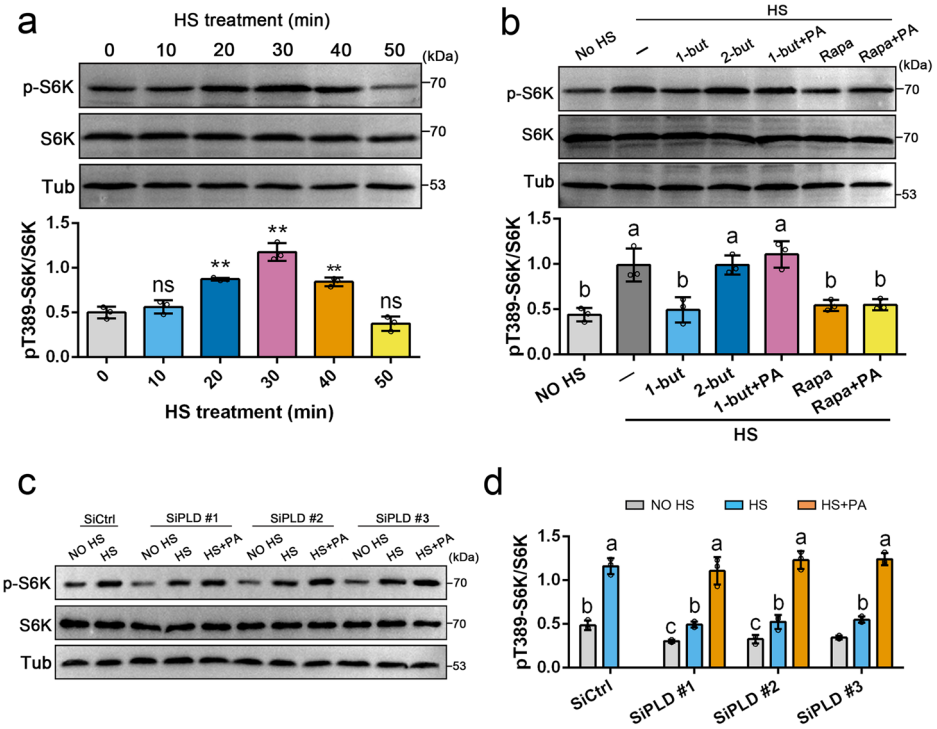

Fig. 3 | Pre-incubation with 1-butanol or silencing of PLD decreases HS-activated mTOR. a Western blot analysis of the phosphorylation states of S6K after HS treatment from 5-d-old WT mycelia. **b** Western blot analysis of the phosphorylation states of S6K. The mycelia were pre-incubated with 0.3% 1-butanol (1-but), 0.3% 2-butanol (2-but), 100 nM rapamycin (Rapa), or 50 μg/100 mL PA for 30 min before being exposed to HS for 30 min. The histogram in (**a**) and (**b**) shows the relative ratio of p-T389-S6K/S6K. p-T389-S6K: phosphorylated S6K at Thr389. **c** Western blot analysis of the phosphorylation states of S6K after 30 min HS treatment from 5-d-old SiControl and *pld*-silenced mycelia. The *pld*-silenced mycelia were incubated with 50 μg/100 mL PA for 30 min before being exposed to HS. **d** The histogram shows the relative ratio of p-T389-S6K/S6K of (**c**). The S6K protein level in the WT or SiControl strain under no HS treatments was arbitrarily set to 1. The values are the means ± SD ($n = 3$ independent experiments). Asterisks in (**a**) indicate significant differences from the no HS treatments (**$P < 0.01$ by Student's *t*-test); ns not significant. Different letters in (**b**) and (**d**) indicate significant differences between the lines ($P < 0.05$, according to Duncan's multiple range test).

anti-mTOR antibody to immunoprecipitate mTOR from *G. lingzhi* mycelia (HS Anti+; Fig. 2a). Lipid analysis revealed that a significantly ($P < 0.05$) greater amount of PA was detected in the sample immunoprecipitated from the HS Anti+ group than in the non-HS-treated group (Anti+; Fig. 2b). PA profiling by mass spectrometry revealed that more 34:0-PA, 34:1-PA, 34:2-PA, 36:2-PA, 36:3-PA and 36:4-PA species interacted with mTOR under HS (Fig. 2c).

In mammals and yeast, rapamycin forms a gain-of-function complex with the FRB domain, which directly interacts with and inhibits mTOR[33,34]. The preceding results suggested that the FRB domain of mTOR was responsible for the interaction with PA, and HS promoted the interaction between PA and mTOR in *G. lingzhi*. Therefore, we further analysed the effect of rapamycin on the PA-FRB interaction under HS in *G. lingzhi*. After preincubation with exogenous rapamycin for 30 min before HS, the lipids that coprecipitated with mTOR were analysed by mass spectrometry. Preincubation with rapamycin did not prevent the isolation of mTOR according to immunoblotting using an anti-mTOR antibody (Rapa+HS Anti+; Fig. 2a). However, rapamycin led to a significant decrease ($P < 0.05$) of ~77.8% in the total PA contents compared to non-rapamycin treatment under HS (Fig. 2b). PA profiling by mass spectrometry revealed that fewer 34:0-PA, 34:1-PA, 34:2-PA, 36:2-PA, 36:3-PA and 36:4-PA species interacted with mTOR when preincubated with rapamycin under HS. These results suggested that a competitive relationship existed between PA and rapamycin in the interaction with the FRB domain of mTOR in *G. lingzhi*.

Activation of the mTOR signalling pathway is dependent on PLD and PA under heat stress

The preceding results suggest that an enhanced interaction between PA and mTOR occurs under HS. We further determined the effect of PLD and PA on the mTOR signalling pathway under HS by detecting ribosomal subunit S6 kinase (S6K), which is one of the best-known downstream effectors of mTOR. We observed that treatment with HS stimulated the phosphorylation of S6K (p-S6K) in the *G. lingzhi* wild-type (WT) strain. The p-S6K/S6K ratio increased ~2.35-fold under HS for 30 min compared to non-HS treatment (Fig. 3a). 1-Butanol is an inhibitor of PA production by PLD because PLD transfers the phosphatidyl group to primary alcohols to produce phosphatidyl alcohol at the expense of PA[35,36]. Functionally, pharmacologically inhibited PLD-mediated formation of PA by 1-butanol abolished HS-stimulated p-S6K. As a control, 2-butanol, which is not a substrate of PLD, was used, and it did not have an inhibitory effect on p-S6K (Fig. 3b). We applied PA to 1-butanol-treated cells to determine whether this treatment prevented the decrease in p-S6K. As shown in Fig. 3b, preexposure to PA prevented the decrease in the HS-induced increase in p-S6K in 1-butanol-treated cells (Fig. 3b), which is consistent with the effect of 1-butanol on PLD. In addition, preincubation with rapamycin decreased HS-induced p-S6K accumulation, but the loss of cytoplasmic p-S6K accumulation evoked by HS in the presence of rapamycin was not reversed by exogenous PA (Fig. 3b), which is consistent with the effect of rapamycin on mTOR activity. These results suggest a competitive relationship between PA and rapamycin in the interaction with the FRB domain of mTOR (Fig. 2).

To further elucidate the role of PLD and PA in regulating the mTOR signalling pathway under HS conditions, the p-S6K levels of *pld*-silenced strains were determined under HS conditions. Genetic silencing of the PLD gene by RNA interference unsensitized p-S6K under HS. Treatment of *pld*-silenced strains SiPLD#1, SiPLD#2 and SiPLD#3 with HS led to ~1.63-, 1.60- and 1.59-fold increases ($P < 0.05$), respectively, in the p-S6K/S6K ratio compared to the non-HS-treated samples. However, the p-S6K levels of the *pld*-silenced strains were significantly lower than those of the SiControl strain under HS. The p-S6K/S6K ratio of SiPLD#1, SiPLD#2 and SiPLD#3 was significantly ($P < 0.05$) reduced by ~57.47%, 54.89%, and 52.59%, respectively, compared to those of the SiControl strain under HS. In addition, when PA was added to the *pld*-silenced strains under HS, the p-S6K level did not significantly differ ($P > 0.05$) between the SiControl strain under HS and the *pld*-silenced strains under HS-PA cotreatment (Fig. 3c, d). These results indicated that PLD-mediated formation of PA was involved in HS-stimulated p-S6K.

The PLD-mediated PA-interacting protein mTOR regulates HS-induced GA biosynthesis

We then asked whether the PLD-mediated PA-interacting protein mTOR was essential for GA biosynthesis under HS. To address this question, we determined the GA content by inhibiting PLD or mTOR under HS

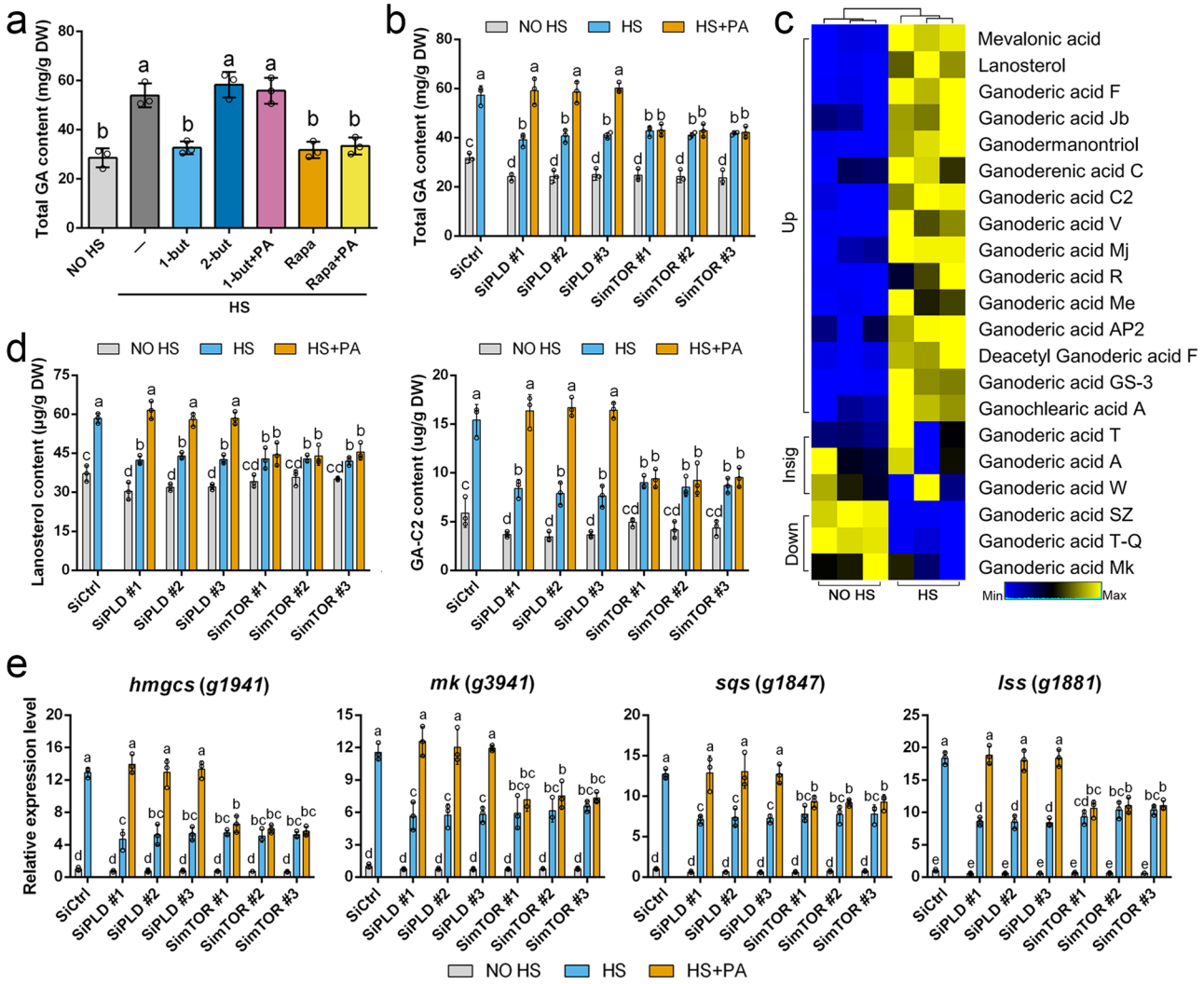

Fig. 4 | PLD mediated PA regulates HS-induced GA biosynthesis by interacting protein mTOR. a Exogenous 1-butanol and rapamycin revert the increased GA content elicited by HS in WT strains. 5-d-old WT strains were incubated with 0.3% 1-butanol (1-but), 0.3% 2-butanol (2-but), 100 nM rapamycin (Rapa), or 50 μg/100 mL PA for 30 min before being exposed to 42 °C for 12 h, and then recovered until the 7th day. **b** Total GA content in SiControl, *pld*- and *mTOR*-silenced strains. The *pld*- and *mTOR*-silenced strains incubated with 50 μg/100 mL PA for 30 min, exposed to HS at shaking for 5 days, and then recovered until the 7th day. **c** Heatmap showing the changes in the contents of detected GAs in no HS and HS of WT strains (three replicas of a single WT strain for each treatment). Up, Down and Insig were indicated the significantly upregulated, downregulated and no significantly differential metabolites, respectively, in the HS compared to no HS sample. **d** The contents of cellular lanosterol and GA-C2 in SiControl, *pld*- and *mTOR*-silenced strains. **e** qRT-PCR analyses of key genes in the GA biosynthetic pathway in SiControl, *pld*- and *mTOR*-silenced strains. The expression level of each gene from the SiControl strain under no HS treatments was arbitrarily set to 1. The values in (**a**), (**b**), (**d**), and (**e**) are the means ± SD ($n = 3$ independent experiments). Different letters indicate significant differences between the lines ($P < 0.05$, according to Duncan's multiple range test).

conditions. As shown in Fig. 4a, compared with the non-HS treatment, HS treatment increased ($P < 0.05$) the GA content by ~1.89-fold in the WT strain. When 1-butanol was added, the GA content did not significantly differ ($P > 0.05$) between the HS-1-butanol cotreated and non-HS-treated samples. However, 2-butanol did not have an inhibitory effect on the GA content under HS treatment. Preincubation with rapamycin for 30 min decreased HS-induced GA accumulation. The GA content following treatment of the samples with rapamycin was significantly lower ($P < 0.05$) than in the absence of rapamycin under HS. Furthermore, exogenous PA rescued the loss of HS-induced GA accumulation in the presence of 1-butanol but not rapamycin (Fig. 4a), which is consistent with the effects of 1-butanol and rapamycin on PLD and mTOR activity, respectively.

We next compared the effects of PA on the GA content in *pld*- and *mTOR*-silenced strains under HS conditions. The HS-induced increase in GA content was considerably reduced in the *pld*- and *mTOR*-silenced strains. In addition, PA increased GA accumulation in the *pld*-silenced strains but not in the *mTOR*-silenced strains under HS conditions (Fig. 4b). Targeted secondary metabolic profiling revealed that the levels of mevalonic acid, lanosterol, and 13 different GAs were significantly greater in the HS samples than in the non-HS samples (Fig. 4c and Supplementary Data 3). In addition, the lanosterol and GA-CA2 contents were lower ($P < 0.05$) in the *pld*- and *mTOR*-silenced strains compared to the SiControl strain after exposure to HS, and this difference returned to the SiControl level after the addition of PA to the *pld*-silenced strains but not to the *mTOR*-silenced strains (Fig. 4d).

The gene expression of the four key enzymes involved in GA biosynthesis, *hmgcs* (encoding 3-hydroxy-3-methylglutaryl CoA synthetase, *g1941*), *mk* (encoding mevalonate kinase, *g3941*), *sqs* (encoding squalene synthase, *g1847*) and *lss* (encoding lanosterol synthase, *g1881*), was also lower ($P < 0.05$) in the *pld*- and *mTOR*-silenced strains than the SiControl strain under HS, and this effect was reversed with PA treatment in the *pld*-silenced strains but not in the *mTOR*-silenced strains (Fig. 4e). These results

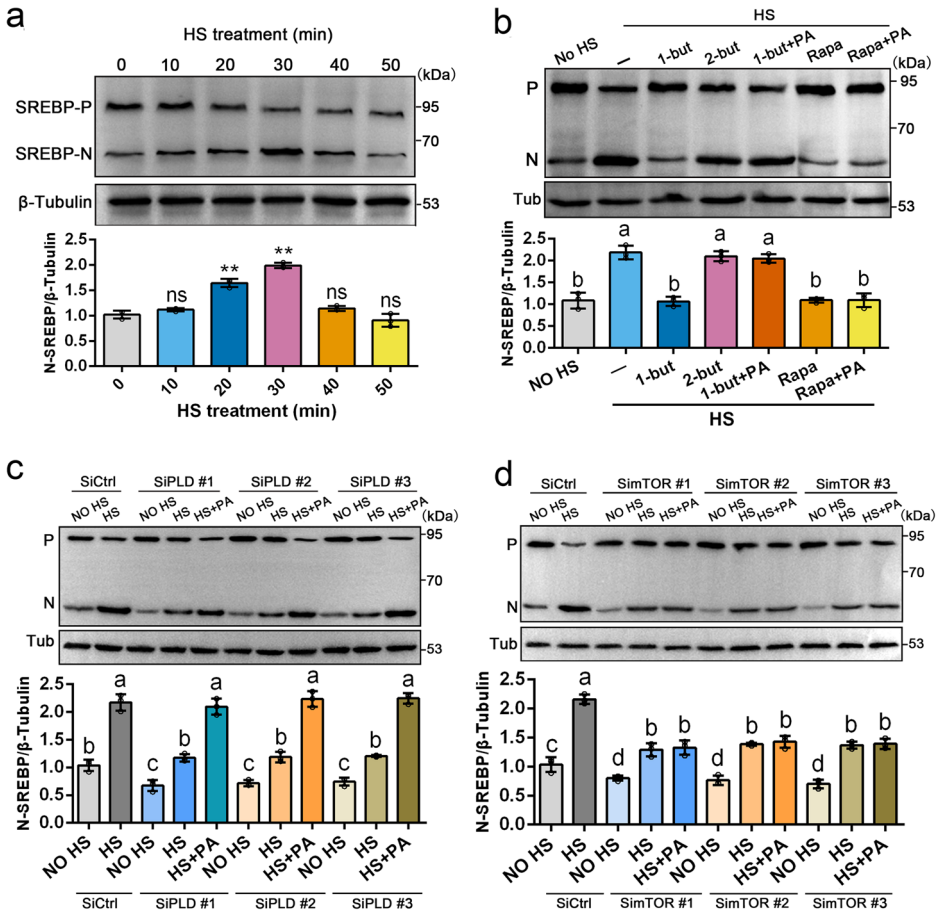

Fig. 5 | mTOR functions downstream of PLD and PA in HS-induced SREBP processing. a Western blot analysis of the SREBP protein levels after HS treatment from 5-d-old WT mycelia. **b** Western blot analysis of the SREBP protein levels. The 5-d-old WT mycelia were pre-incubated with 0.3% 1-butanol (1-but), 0.3% 2-butanol (2-but), 100 nM rapamycin (Rapa), or 50 μg/100 mL PA for 30 min before being exposed to HS for 30 min. **c**, **d** Western blot analysis of the protein levels of SREBP after 30 min HS treatment from 5-d-old SiControl, *pld*- and *mTOR*-silenced strains. The *pld*- and *mTOR*-silenced strains were incubated with 50 μg/100 mL PA for 30 min before being exposed to HS. **a**–**d** P and N denote the full-length, precursor SREBP and the cleaved, active SREBP, respectively. The histogram in (**a**–**d**) shows the N-SREBP/β-Tubulin ratio which in the WT or SiControl strain under no HS treatments was arbitrarily set to 1. The values are the means ± SD ($n = 3$ independent experiments). Asterisks in (**a**) indicate significant differences from the no HS treatments (**$P < 0.01$ by Student's *t*-test); ns: not significant. Different letters in (**b**–**d**) indicate significant differences between the lines ($P < 0.05$, according to Duncan's multiple range test).

suggest that PLD-mediated PA regulates HS-induced GA biosynthesis by interacting with the protein mTOR.

Activation of the nuclear form of SREBP is dependent on the PLD-mediated PA-interacting protein mTOR under heat stress

Next, we asked how mTOR regulated GA biosynthesis under HS, i.e., what is the intermediate downstream of mTOR that regulates GA biosynthesis? One possible candidate intermediate is the transcription factor SREBP, which directly activated GA biosynthesis in our previous report[32]. Studies in animals demonstrated that SREBP transport from ER to the Golgi apparatus where two proteases sequentially cleave and release its transcription factor domain for translocation to the nucleus[37]. And mTOR was required for the increase in SREBP cleavage and stimulation of its target genes[38,39].

To investigate the role of PLD, PA and mTOR at the protein level, the SREBP protein level was analysed under HS treatment. Western blot analysis revealed increased levels of the nuclear form of SREBP (N-SREBP) protein after exposure to HS. The N-SREBP protein level significantly ($P < 0.01$) increased by ~1.61- and 1.95-fold at 20 and 30 min, respectively, under HS conditions in *G. lingzhi* (Fig. 5a). Next, we applied 1-butanol or rapamycin to HS-treated cells to determine whether this treatment prevented the increase in N-SREBP levels. As shown in Fig. 5b, preexposure to 1-butanol or rapamycin prevented the increase in the N-SREBP level under HS. Furthermore, exogenous PA rescued the loss of N-SREBP accumulation induced by HS in the presence of 1-butanol but not rapamycin. These results suggest that PLD- and PA-mediated mTOR activity are necessary for HS-induced increases in N-SREBP levels.

We used genetic tests to verify the functions of the PLD-mediated PA-interacting protein mTOR in the processing of SREBP under HS conditions. Treatment with HS increased N-SREBP levels in the SiControl strain, but this increase was greatly reduced in the *pld*- and *mTOR*-silenced strains (Fig. 5c, d). In the SiControl strain, treatment with HS led to an increase ($P < 0.05$) of ~2.09-fold in the N-SREBP levels compared to non-HS treatment, and treatment of the *pld*- and *mTOR*-silenced strains with HS led to an increase ($P < 0.05$) of ~1.67-fold and 1.78-fold, respectively, in the N-SREBP levels compared to the non-HS-treated samples. The N-SREBP levels of the *pld*- and *mTOR*-silenced strains were significantly lower than those of the SiControl strain under HS. In addition, the application of PA increased the N-SREBP protein level in *pld*-silenced strains but not in *mTOR*-silenced strains (Fig. 5c, d). These data indicated that PLD and PA were involved in HS-induced SREBP processing, and mTOR functioned downstream of PLD and PA.

SREBP acts downstream of PLD, PA, and mTOR in HS-induced GA biosynthesis

We then asked whether SREBP was an intermediate of the PLD-mediated PA-interacting protein mTOR in HS-induced GA biosynthesis. Fatostatin impairs the activation of SREBP by avoiding SREBP transport from ER to the Golgi[40,41]. Functionally, pharmacological inhibition of SREBP activity by 10 μM fatostatin abolished HS-stimulated GA biosynthesis and N-SREBP levels (Fig. 6a and Supplementary Fig. 2). Moreover, exogenous PA did not rescue the loss of HS-induced GA accumulation in the presence of fatostatin (Fig. 6a).

We used genetic tests to verify the functions of SREBP in GA biosynthesis under HS. As shown in Fig. 6b, treatment of the SiControl strain with HS led to increases ($P < 0.05$) of ~2.08-, 1.93- and 3.00-fold in the total GA, lanosterol and GA-C2 content, respectively, compared to the non-HS treatment, and treatment of *SREBP*-silenced strains with HS led to increases ($P < 0.05$) of ~1.43-, 1.794- and 2.11-fold in the total GA, lanosterol and GA-C2 content, respectively, compared to the non-HS treatment. The total GA, lanosterol and GA-C2 contents of the *SREBP*-silenced strains were

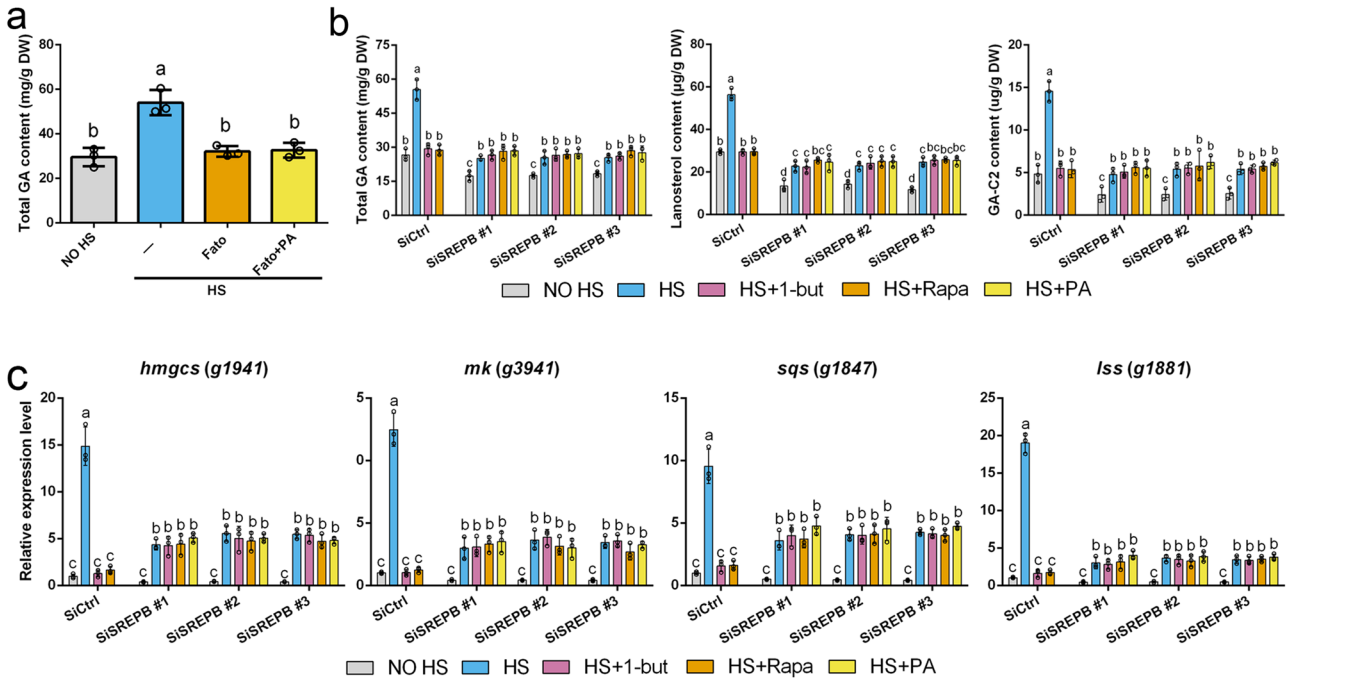

Fig. 6 | SREBP acts downstream of PLD mediated PA interacting protein mTOR in HS-induced GA biosynthesis. a Exogenous fatostatin (Fato) abolish the total GA content increment elicited by HS in WT strains, and this could not be reverted by PA addition. **b** The contents of cellular total GA, lanosterol and GA-C2 in SiControl and *SREBP*-silenced strains. **c** qRT-PCR analyses of key genes in the GA biosynthetic pathway in SiControl and *SREBP*-silenced strains. The expression level of each gene from the SiControl strain under no HS treatments was arbitrarily set to 1. **a**–**c** 5-d-old WT, SiControl or *SREBP*-silenced strains were incubated with 10 μM fatostatin (Fato), 50 μg/100 mL PA, 0.3% 1-butanol (1-but) or 100 nM rapamycin (Rapa) before being exposed to HS and then recovered. The values are the means ± SD ($n = 3$ independent experiments). Different letters indicate significant differences between the lines ($P < 0.05$, according to Duncan's multiple range test).

significantly lower than the SiControl strain under HS, and this effect was not reversed with PA treatment in the *SREBP*-silenced strains. Furthermore, the gene expression of *hmgcs*, *mk*, *sqs* and *lss* was also lower ($P < 0.05$) in the *SREBP*-silenced strains than in the SiControl strain under HS, and this effect was not reversed with PA treatment in the *SREBP*-silenced strains (Fig. 6c). These results suggest that SREBP is involved in HS-induced GA biosynthesis and functions downstream of PA.

Next, we further validated that SREBP acts downstream of PLD and mTOR in HS response and HS-induced GA biosynthesis. Western blot analysis revealed that HS produced a significant increase ($P < 0.01$) of ~2.84-fold in the p-S6K/S6K compared to the non-HS treatment in the *SREBP*-silenced strains. The p-S6K level was not significantly different ($P > 0.05$) between SiControl and *SREBP*-silenced strains under HS and non-HS treatment (Fig. 7a). In addition, 1-butanol or rapamycin could abolish HS-stimulated p-S6K in the *SREBP*-silenced strains (Fig. 7a). These results showed that SREBP silencing did not block HS activated mTOR activity, and indicated that SREBP acts downstream of PLD and mTOR in HS response. Moreover, 1-butanol or rapamycin could considerably reduce the HS-induced increase in total GA, lanosterol, and GA-C2 accumulation and *hmgcs*, *mk*, *sqs* and *lss* expression in the SiControl strain, but could not in the *SREBP*-silenced strains (Fig. 6b, c). These results indicated that SREBP acts downstream of PLD and mTOR in HS-induced GA biosynthesis.

Our previous experimental evidence of DNA affinity purification sequencing and EMSA have suggested the *hmgcs* and *mk* are direct targets of SREBP[32]. Here we conducted a bioinformatic promoter analysis for SREBP binding sites of the *sqs* and *lss* genes (Fig. 7b, Supplementary Fig. 3 and Supplementary Tables 1 and 2). EMSA showed that SREBP caused a gel shift of sqs_{pro} and lss_{pro}, and a weakened shift was detected when unlabelled DNA was added. This binding activity vanished upon motif mutation (Fig. 7b). These results, combined with previous experimental evidence[32], indicate that the four key GA biosynthesis genes are direct targets of SREBP. Collectively, our results suggested that SREBP was key for signal transmission, and SREBP processing was an intermediate of the PLD-mediated PA-interacting protein mTOR in HS-induced GA biosynthesis in *G. lingzhi*.

Overall, HS promotes the direct binding of PA to mTOR and the activation of the mTOR signalling pathway, which was abolished by rapamycin. PA rescued the reduction in mTOR activity and GA biosynthesis in the presence of 1-butanol and in *pld*-silenced strains, but not in the presence of rapamycin or in *mTOR*-silenced strains under HS. PA rescued the reduction in the nuclear form of SREBP in the presence of 1-butanol and in *pld*-silenced strains, but not in the presence of rapamycin or in *mTOR*-silenced strains under HS. Moreover, PA did not rescue the decrease in GA biosynthesis in the presence of fatostatin or in *SREBP*-silenced strains under HS. Notably, SREBP silencing did not block HS-stimulated mTOR activity. In addition, 1-butanol or rapamycin abolished HS-stimulated mTOR activity, but not HS-stimulated GA biosynthesis, in *SREBP*-silenced strains. Therefore, our results suggest that PLD-mediated PA directly activates mTOR and regulates SREBP to promote the transcription of SREBP target genes and GA biosynthesis under HS in *G. lingzhi*.

Discussion

As important secondary metabolites of *Ganoderma*, GAs exhibit broad-spectrum pharmacological potential[2,3]. The increasing commercial importance of GAs has resulted in great interest in their biosynthesis. Environmental stress often triggers perturbations in the biosynthesis of metabolites. HS is one of the most important environmental abiotic stresses, and it significantly affects the growth and secondary metabolism of organisms[19,42]. Our previous studies revealed that PLD-mediated PA signalling molecules were involved in HS-induced GA biosynthesis[21]. However, the underlying mechanism of the 'membrane signals' involved in the response to HS and the regulation of GA biosynthesis is unclear. This study found that HS stimulated PA binding to and activation of mTOR, which enhanced cytosolic, precursor SREBP processing to the nuclear form of SREBP, which directly regulated GA biosynthesis (Fig. 8). Our report established the link between PLD-mediated PA production and the activation of mTOR and

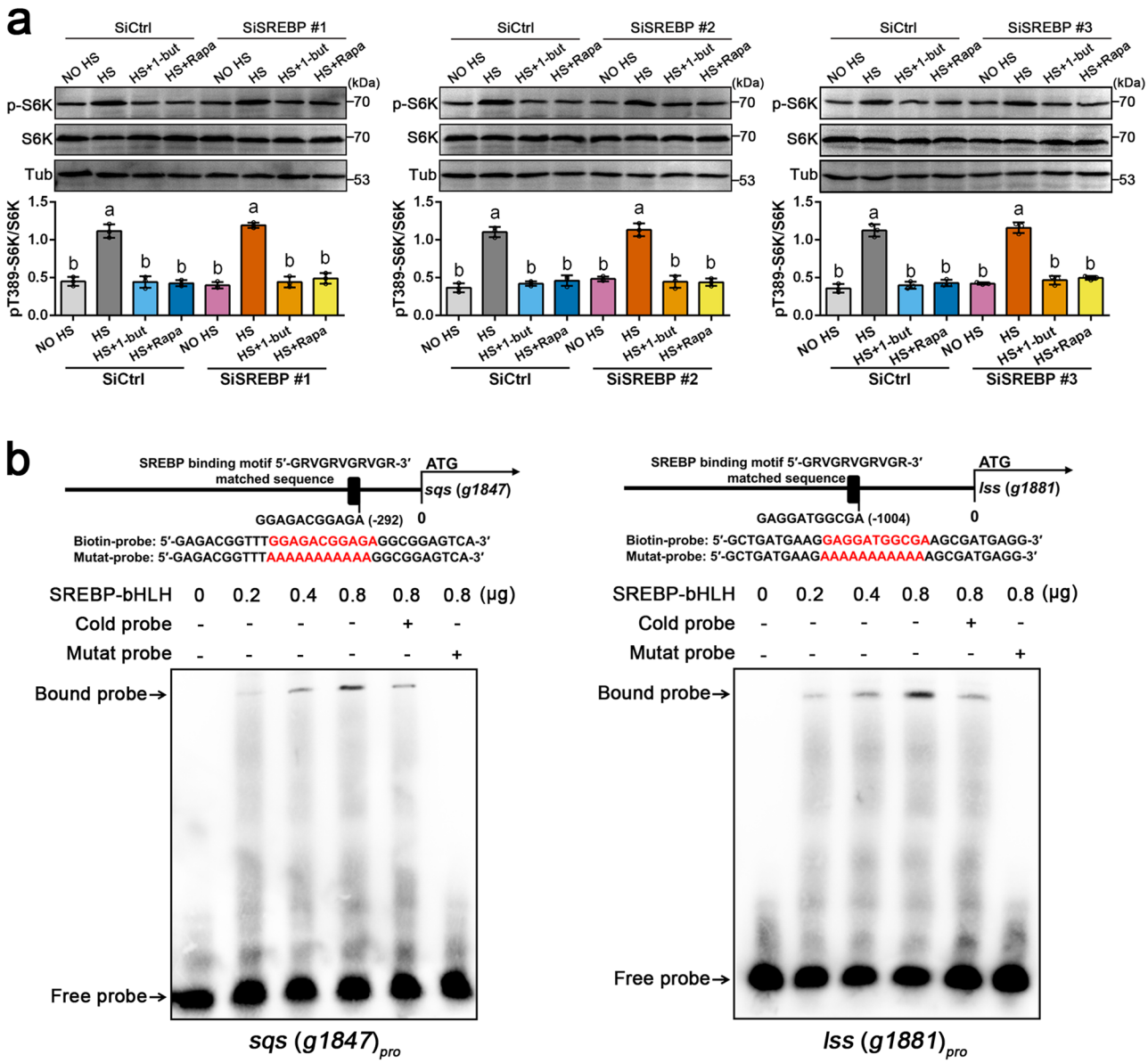

Fig. 7 | HS could activate mTOR activity in *SREBP*-silenced strains, but this activation could be removed by 1-butanol or rapamycin. a Western blot analysis of the phosphorylation states of S6K after HS treatment 30 min from 5-d-old SiControl and *SREBP*-silenced strains. The *SREBP*-silenced strains incubated with 0.3% 1-butanol (1-but) or 100 nM rapamycin (Rapa) for 30 min before being exposed to HS. The histogram shows the relative ratio of p-T389-S6K/S6K, and the protein level of the S6K in the SiControl strain under no HS treatments was arbitrarily set to 1. p-T389-S6K: phosphorylated S6K at Thr389. The values are the means ± SD ($n = 3$ independent experiments). Different letters indicate significant differences between the lines ($P < 0.05$, according to Duncan's multiple range test). **b** Binding of SREBP to the promoter of *sqs* and *lss* genes according to the EMSA analysis.

SREBP in the HS response and HS-induced secondary metabolism in filamentous fungi.

Understanding how organisms sense temperature and integrate this information into their development and metabolism is important for determining how organisms adapt to climate change and for applying this knowledge to breeding. The regulatory network involved in thermomorphogenesis, including heat shock factor and reactive oxygen species scavenging, elicits rapid increases in cytosolic Ca^{2+} and has been well established in Arabidopsis[43]. This network is also involved in HS-induced GA biosynthesis[18,19,22]. mTOR signalling is involved in HS responses in animals[44]. For example, mTOR signalling is coupled to heat-induced stress granules to protect cells from DNA damage[45]. mTOR-mediated liquid-liquid phase separation acts as a switch-like HS sensor that couples phase separation to autophagic degradation and adaptation to HS during development[46]. However, the molecular mechanism of HS activation of mTOR has not been fully elucidated, and there is limited research on the HS response of mTOR in plants and microorganisms. The first demonstration that PA was involved in the regulation of mTOR was that exogenously provided PA bound directly to the FRB domain and activated mTOR in Homo sapiens HEK293 cells[25]. Structural studies revealed that PA interacted with the FRB domain and caused structural changes similar to rapamycin-FKBP12 binding to the FRB domain[47]. A structural study also examined the interaction between FRB and PA-rich membranes[48], and the FRB domain of mTOR bound to PA to promote mTOR complex assembly and stability[49]. The growth factor stimulation of mTOR also requires PA[50]. However, little is known about the interaction between the FRB domain of mTOR and PA under the HS response. This study also found that the *G. lingzhi* FRB domain bound to PA, which is consistent with the finding that FRB

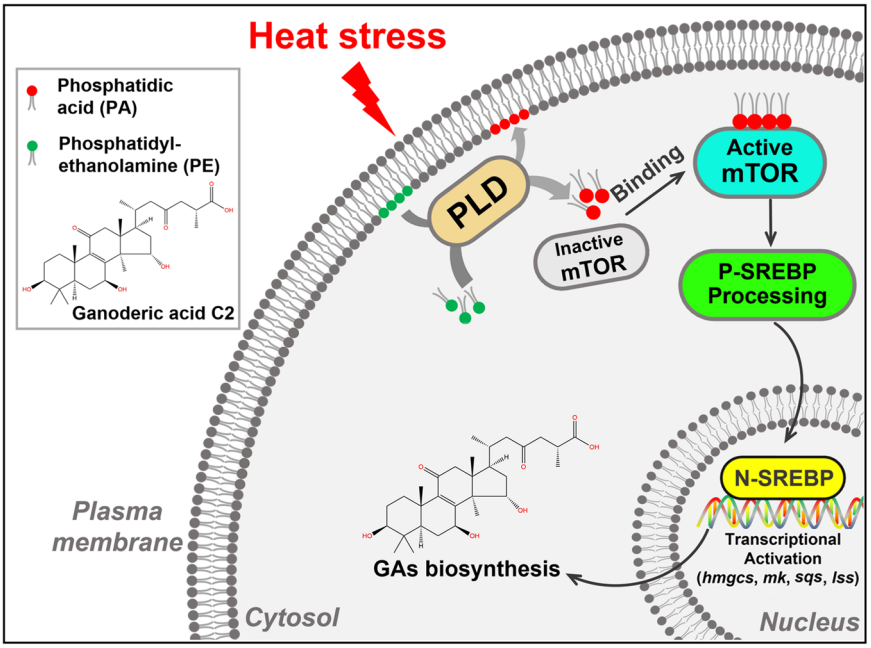

Fig. 8 | Model depicting the role of PLD, PA, mTOR and SREBP in HS-induced GA biosynthesis in *G. lingzhi*. When cells exposure to HS, the PLD activity is increased and generates second lipid messengers PA. PA binds to and activates mTOR, and then enhance cytosolic, precursor SREBP processing to nuclear form of SREBP. N-SREBP promoted the transcription of its target genes *hmgcs*, *mk*, *sqs*, *lss*, and further GA biosynthesis. The representative GAs (GA-C2) is displayed.

sequences are conserved in animals and fungi. More importantly, our study revealed that HS stimulated PA binding to mTOR, which was sufficient for mTOR catalytic activity in *G. lingzhi*.

The competitive regulation of mTOR activity by PA and mTOR has received widespread interest and research. Suppressing PA production substantially increased the sensitivity of mTOR to rapamycin[51]. Incubation with the FKBP12-rapamcyin complex effectively eliminated PA binding to FRB[25]. Elevated PLD activity in human breast cancer cells increased the concentration of rapamycin required to suppress mTOR[52]. In agreement with the competitive nature between PA and rapamycin, binding of rapamycin-FKBP12 to FRB prevents the domain from interacting with PA-rich membranes at lower lipid concentrations (lower than 10 mM), but can be overcome by high lipid concentrations (higher than 10 mM)[48]. Our results show that exogenous PA (50 μg/100 mL, approximately equal to 0.75 μM) not reverse the effect of rapamycin (100 nM), which may be due to the lower concentration of PA (Figs. 3b and 4a). It has been reported that a higher concentration of PA (100 μM) could reverse the effect of 200 nM rapamycin on mTOR activity[51].

SREBP is conserved in mammals, worms, flies, and yeast and functions in the regulation of sterol homoeostasis and lipid metabolism[53]. Through unknown mechanisms, mTOR promotes the function of SREBP. Hyperactive mutation of mTOR signalling protects cancer cells from oxidative stress and ferroptotic death via SREBP-mediated lipogenesis[41]. Mammalian mTOR regulates SREBP by controlling the nuclear entry of lipin 1, a phosphatidic acid phosphatase[54]. SREBP processing is increased upon stimulation of the mTOR signalling pathway, which leads to an increase in the transcription of lipogenic genes[38]. In addition, inhibition of S6K blocked the insulin-dependent increase in the nuclear form of SREBP, but the mechanisms by which S6K leads to SREBP cleavage are not known[55]. The two-step process by which SREBP regulates lipid homeostasis has been well established in animal cells. When cellular cholesterol levels fall below a threshold (5% of total ER lipids, molar basis)[56], Scap escorts SREBP from the ER to the Golgi, where SREBP is sequentially cleaved by two Golgi-resident proteases, site-1 and site-2 protease, which release its carboxyl-terminal transcription factor domain from the membrane for translocation to the nucleus to upregulate the expression of lipogenic genes[57,58]. *Dsc-2* and *tul-1* in the fungi *Schizosaccharomyces pombe* and *Aspergillus fumigatus* are components of the Golgi apparatus E3 ligase complex, which is critical for the activation of SREBP by proteolytic cleavage[59,60]. In addition, *S. pombe* SREBP upregulates sterol synthesis by targeting the activity of HMG-CoA reductase following HS[61]. Our study revealed that SREBP was involved in the HS response, and the PA-mTOR-SREBP signalling pathway was involved in HS-induced GA biosynthesis. However, further research is needed on how mTOR activates SREBP under HS in *G. lingzhi*.

In summary, the results obtained in this study indicated that HS stimulated PA binding to and activation of mTOR. Activation of the nuclear form of SREBP was dependent on the PLD-mediated PA-interacting protein mTOR under HS. Finally, SREBP acted downstream of PLD, PA, and mTOR in HS-induced GA biosynthesis by promoting the transcription of its target genes *hmgcs*, *mk*, *sqs* and *lss*.

Methods

Fungal strains and culture conditions

The *G. lingzhi* strain SCIM 1006 (NO. CGMCC 18819) was cultured on artificial medium with shaking at 160 rpm in the dark. The culture medium was composed of the following: 2% glucose, 1% maltose, 0.05% $MgSO_4$. $7H_2O$, 0.2% yeast extract, 0.46% KH_2PO_4 and 0.2% tryptone.

HS treatments and chemical treatments

The HS treatments were conducted according to a protocol described previously with some modifications[19]. To evaluate the SREBP and S6K protein levels, 5-day-old mycelia were heat stressed at 42 °C in a temperature-controlled chamber. To detect GA and its mesostate, after shaking for 5 days, the mycelia were exposed to 42 °C for 12 h and then recovered until the 7th day at 28 °C in stationary liquid cultures.

In the experiments in which chemical reagent was used, the mycelia were incubated with the concentrations of 1-butanol, 2-butanol, rapamycin, PA or fatostatin indicated in the figure legends for 30 min before HS treatment.

Enrichment and identification of PA binding proteins

The 5-d-old *G. lingzhi* mycelia were harvested and washed once with PBS and lysed on ice in 5 volumes of a 10 mM HEPES, pH 7.4, 1.5 mM $MgCl_2$ and 10 mM KCl in a homogenizer. PA beads were obtained from Echelon Biosciences Inc (Echelon Inc, Salt Lake City, USA, P-B0PA). Beads were washed five times with 10 volumes of washing buffer (10 mM HEPES, pH 7.4, 150 mM NaCl, 0.25% Igepal). Incubate the protein-bead solution at 4 °C and continuous motion to keep beads in suspension. PA binding proteins

were eluted by boiling PA beads in 2X Laemmli Sample Buffer at 95 °C for 10 min. Proteins were resolved on SDS-PAGE. The gel was stained with colloidal Coomassie blue, cut into 20 slices and processed for mass spectrometric analysis as described before[31,62]. Cysteines were reduced with dithiothreitol (DTT) and alkylated using chloroacetamide. Proteins were digested overnight with trypsin. The digested peptides were run on the LC tandem MS using an LTQ-Orbitrap Velos mass spectrometer (Thermo Fisher Scientific) coupled with a U3000 RSLC nano HPLC (ThermoFisher Scientific). The database search was performed with peptide mass fingerprint data using MASCOT (v2.4) database search engine (Matrix Science) against the NCBI database (PRJNA738334) for *G. lingzhi*.

Pulldown of specific PA binding protein mTOR

For validation of specific PA binding protein mTOR, DNA fragment was cloned into a prokaryotic expression plasmid pGEX 4T-1 introduced into *E. coli*. Purified GST-tagged proteins mTOR and different mTOR domains were incubated with PA beads as described above and analysed by immunoblotting with monoclonal GST antibody B-14 (1:200, Santa Cruz, sc-138). The coding region of mTOR was amplified by PCR using *G. lingzhi* cDNA as a template with the primers listed in Supplementary Table 3.

Western blotting

Polyclonal antibody against SREBP or mTOR was obtained by sent the SREBP-bHLH protein or mTOR-FRB to a professionally qualified antibody preparation company and used for the immunization of rabbits (Chemgen Biotech, Shanghai, China). Antibodies against phospho-S6K (Thr389, 1:1000, #9234), S6K (1:1000, #9202) and β-Tubulin antibody (1:1000, #2146) were purchased from Cell signalling technology (Danvers, MA, USA). Proteins from *G. lingzhi* mycelia were separated in a 12% (w/v) SDS-PAGE gel, transferred to polyvinylidene difluoride membranes (Bio-Rad), and incubated with a primary rabbit antibody (1:2000) and then with a secondary HRP goat anti-rabbit IgG antibody.

Immunoprecipitation and analysis of mTOR-PA complex

Immunoprecipitation was performed using 5-d-old *G. lingzhi* mycelia, an anti-mTOR antibody and Protein A/G Agarose Beads (Engibody, IF0001), according to the manufacturer's instructions. Briefly, the mycelia were ground with liquidnitrogen and incubated in protein extraction buffer (50 mM Tris-HCl, pH 7.3, 50 mM NaCl, 5% glycerol, 1 mM DTT) containing a protease inhibitor cocktail (Sigma-Aldrich) on ice for 1 h. Following brief sonication for membrane disruption, supernatant after centrifugation at 12,000 × *g* for 10 min at 4 °C was used as a protein extract. Then, the protein extract (100 mg total proteins determined by Bradford assay) was incubated with 5 μg antibody against mTOR (anti+) or IgG (anti-) at 4 °C for 12 h with constant rotation. After incubation, 20 μL washed Protein A/G Agarose Beads were transferred to the lysate and incubated at 4 °C overnight with constant rotation. The mixture was washed five times with washing buffer (20 mM NaH_2PO_4 pH 8.0, 150 mM NaCl) by centrifugation at 1500 × *g* for 1 min. For protein-lipid complex analysis, lipids were extracted from the resulting pellet with chloroform/methanol (2:1) mixture, dried under gentle stream of nitrogen gas, and resuspended with chloroform. 0.01 pmol di14:0-PA were added as internal standards. The lipid extracts were analyzed by automated electrospray ionization–tandem mass spectrometry (ESI-MS/MS). In total, 2 μl of solution was injected into the UPLC column (2.1 *100 mm ACQUITY UPLC BEH C18 column containing 1.7 μm particles) with a flow rate of 0.4 ml/min. Buffer A consisted of 0.1% formic acid in water, and buffer B consisted of 0.1% formic acid in acetonitrile. The gradient was 25% Buffer B for 2 min, 25%–95% Buffer B for 15 min, and 95% Buffer B for 2 min. Mass spectrometry was performed using an electrospray source in positive ion mode with MSe acquisition mode, with a selected mass range of 50–1200 *m/z*. The lock mass option was enabled using leucine-enkephalin (*m/z* 556.2771) for recalibration. The ionization parameters were the following: capillary voltage 2.5 kV, collision energy 40 eV, source temperature 120 °C, and desolvation gas temperature 400 °C. Data acquisition and processing were performed using Masslynx 4.1.

Construction of RNAi plasmids and strains

The RNA interference vector was derived from the *Agrobacterium tumefaciens* binary vector pCAMBIA 1300 (CAMBIA, Canberra). Inhibition of gene expression by 35S promoter from CaMV and glyceraldehyde-3-phosphate dehydrogenase (GPD) gene promoter from *G. lingzhi*. The *pld*, *mTOR* and *SREBP* gene was amplified by PCR using *G. lingzhi* cDNA as the template and the primers listed in Supplementary Table 3. This vector was transformed to the *G. lingzhi* strain by *Agrobacterium mefaciens-mediated transformation* (ATMT). The transformants were selected on plate culture medium containing 100 μg/mL hygromycin B. qRT–PCR was performed to detect the gene expression in the WT strain and positive transformants (Supplementary Fig. 4).

Determination of cellular GA, lanosterol and GA-C2 contents

Experimental procedure used here to determine the content of cellular GA, lanosterol and GA-C2 was similar to one used previously[32]. The 7-d-old *G. lingzhi* mycelia with or without HS were used secondary metabolite extraction and mass spectrometry analysis (Fig. 4c). Mycelia samples were freeze-dried by a vacuum freeze-dryer (Scientz-100F). The freeze-dried sample was crushed using a mixer mill (MM 400, Retsch) with a zirconia bead for 1.5 min at 30 Hz. Then, 100 mg of lyophilized powder was dissolved in 1.2 mL 70% methanol solution, vortexed for 30 s every 30 min for a total of 6 times, and finally placed in a refrigerator at 4 °C overnight. Following centrifugation, the extracts were filtered (SCAA-104, 0.22-μm pore size; ANPEL, Shanghai, China) before UPLC–MS/MS analysis (UPLC, Shim-pack UFLC SHIMADZU CBM A system; MS, QTRAP® 4500+ System). The analytical conditions were as follows: UPLC: column, Waters ACQUITY UPLC HSS T3 C18 (1.8 μm, 2.1 mm*100 mm); column temperature, 40 °C; flow rate, 0.4 mL/min; injection volume, 2 μL; solvent system, water (0.1% formic acid): acetonitrile (0.1% formic acid); gradient program, 95:5 V/V at 0 min, 5:95 V/V at 10.0 min, 5:95 V/V at 11.0 min, 95:5 V/V at 11.1 min, and 95:5 V/V at 15.0 min. LIT and triple quadrupole (QQQ) scans were acquired on a triple quadrupole-linear ion trap mass spectrometer (Q TRAP), the AB4500 Q TRAP UPLC/MS/MS System, equipped with an ESI Turbo Ion-Spray interface operating in positive and negative ion mode and controlled by Analyst 1.6.3 software (AB Sciex). The ESI source operation parameters were as follows: ion source, turbo spray; source temperature 550 °C; ion spray voltage (IS) 5500 V (positive ion mode)/-4500 V (negative ion mode); ion source gas I (GSI), gas II (GSII), and curtain gas (CUR) were set at 50, 60, and 25.0 psi, respectively; and collision-activated dissociation (CAD) was high. Instrument tuning and mass calibration were performed with 10 and 100 μmol/L polypropylene glycol solutions in QQQ and LIT modes, respectively. QQQ scans were acquired as MRM experiments with collision gas (nitrogen) set to medium. DP and CE for individual MRM transitions were performed with further DP and CE optimization. A specific set of MRM transitions was monitored for each period according to the metabolites eluted within this period.

For the determination of total GA content, the dried mycelia (2 g) were extracted by circumfluence with 75% (v/v) ethanol (100 mL) for 3 h (twice). After removal of the mycelia by centrifugation, the supernatant was dried under vacuum. The residues were suspended in water and later extracted with chloroform (100 mL) for 2 h (twice). After removal of the chloroform by evaporation, the sample was further extracted with 5% (w/v) $NaHCO_3$ (200 mL) for 12 h, and adding 2 M HCl to adjust the pH to 3. The GAs in the $NaHCO_3$ layer were extracted with chloroform (200 mL) for 12 h. After removal of the chloroform by evaporation, the GAs were then dissolved in absolute ethanol, and their absorbance was measured at 245 nm using ursolic acid as the standard.

For the determination of lanosterol, the lanosterol were extracted with methanol and ethanol (60:40, v/v) (three times). The extracts were saponified with 0.1 M methanolic NaOH at 50 °C for 2 h. The hydrolysed samples were mixed with 2 mL of distilled deionized water and extracted

twice with 5 mL petroleum ether (boiling point range, 60–90 °C). The petroleum ether layer was pooled and evaporated to dryness under a stream of nitrogen. The dry samples were redissolved in 100 µL of methanol and were later injected into an Agilent 1200 series HPLC with an Agilent Zorbax SB-C18 column (250 × 4.6 mm, 5 µm). The detector was set at 282 nm. Chromatographic peaks were identified by comparing the retention times and spectra against the standards of lanosterol (≥98%, MedChemExpres)[13].

For the measurement of individual ganoderic acids (GA-C2), 100 mg dried mycelia were extracted with methanol, and the GA-C2 in the supernatant were monitored at 254 nm by HPLC using an Agilent 1200 series HPLC with an Agilent Zorbax SB-C18 column (250 × 4.6 mm, 5 µm). The calibration curve for the measurement of GA-C in the fungal mycelia were constructed using the standards of GA-C2 (>99%, MedChemExpress)[63].

Real-time quantitative PCR analysis of gene expression

The levels of gene-specific mRNA expressed were assessed using qRT-PCR. Total RNAs were separately extracted and reversed into cDNAs. Gene expression was evaluated by calculating the difference between the threshold cycle (CT) value of the gene analysed and the CT value of the housekeeping gene 18S rRNA. qRT-PCR calculations analysing the relative gene expression levels were performed according to the $2^{-\Delta\Delta CT}$ method with paired primes listed in Supplementary Table 3.

Electrophoretic mobility gel shift assay (EMSA)

EMSA was performed using the Lightshift Chemiluminescent EMSA Kit (Thermo Scientific, 20148) according to the manufacturer's instructions. The SREBP-bHLH proteins were obtained by prokaryotic expression and purification similar to our previous research[32]. In parallel, nucleotide sequences were biotin labelled at the 3′ end using an EMSA Probe Biotin Labelling Kit (Beyotime, Nantong, China). Unlabelled probes were subjected to cold competition experiments. The nucleotide sequences of probes used are shown in Supplementary Table 3. The biotin signals were imaged using the ChemiDoc MP Imaging System (Bio–Rad Laboratories, Inc., Hercules, CA, USA).

Statistics and reproducibility

All data presented in this manuscript are from three independent experiments. Error bars indicate standard deviation from the mean from triplicate independent experiments. Two methods were used to analyse the significance of the data. Asterisks indicate significant differences ($^{**}P < 0.01$) compared to the control according to Student's *t*-test. Different letters indicate significant differences between the lines ($P < 0.05$) according to Duncan's multiple range test.

Reporting summary

Further information on research design is available in the Nature Portfolio Reporting Summary linked to this article.

Data availability

All data generated or analyzed during this study are included in this published article and its Supplementary Information files. The source data underlying the graphs in the figure are shown in Supplementary Data 4. Uncropped western blots are in Supplementary Figs. 5–9.

Received: 2 July 2024; Accepted: 6 November 2024;
Published online: 13 November 2024

References

1. Ren, A. et al. Shedding light on the mechanisms underlying the environmental regulation of secondary metabolite ganoderic acid in *Ganoderma lucidum* using physiological and genetic methods. *Fungal Genet. Biol.* **128**, 43–48 (2019).
2. Shiao, M. S. Natural products of the medicinal fungus *Ganoderma lucidum*: occurrence, biological activities, and pharmacological functions. *Chem. Record* **3**, 172–180 (2003).
3. Liang, C. et al. Review of the molecular mechanisms of *Ganoderma lucidum* triterpenoids: ganoderic acids A, C2, D, F, DM, X and Y. *Eur. J. Med. Chem.* **174**, 130–141 (2019).
4. Calviño, E. et al. *Ganoderma lucidum* induced apoptosis in NB4 human leukemia cells: involvement of Akt and Erk. *J. Ethnopharmacol.* **128**, 71–78 (2010).
5. Li, Y. et al. Discovery of ganoderic acid A (GAA) PROTACs as MDM2 protein degraders for the treatment of breast cancer. *Eur. J. Med. Chem.* **270**, 116367 (2024).
6. Lv, X. C. et al. Ganoderic acid A from *Ganoderma lucidum* protects against alcoholic liver injury through ameliorating the lipid metabolism and modulating the intestinal microbial composition. *Food Funct.* **13**, 5820–5837 (2022).
7. Sato, N., Zhang, Q., Ma, C.-M. & Hattori, M. Anti-human immunodeficiency virus-1 protease activity of new lanostane-type triterpenoids from *Ganoderma sinense*. *Chem. Pharm. Bull.* **57**, 1076–1080 (2009).
8. Jiang, L. et al. Transcriptome profiling and bioinformatic analysis of the effect of ganoderic acid T prevents Sendai virus infection. *Gene* **862**, 147252 (2023).
9. Quan, Y. Z. et al. Ganoderic acids alleviate atherosclerosis by inhibiting macrophage M1 polarization via TLR4/MyD88/NF-κB signaling pathway. *Atherosclerosis* **391**, 117478 (2024).
10. Yu, Z. R. et al. Ganoderic acid A protects neural cells against NO stress injury in vitro via stimulating β adrenergic receptors. *Acta Pharmacol. Sin.* **41**, 516–522 (2020).
11. Cui, J. et al. Ganoderic acids A and B reduce okadaic acid-induced neurotoxicity in PC12 Cells by inhibiting tau hyperphosphorylation. *Biomed. Environ. Sci.* **36**, 103–108 (2023).
12. Zhao, X. R. et al. Isolation and identification of oxygenated lanostane-type triterpenoids from the fungus. *Phytochem. Lett.* **16**, 87–91 (2016).
13. Xu, J. W., Xu, Y. N. & Zhong, J. J. Production of individual ganoderic acids and expression of biosynthetic genes in liquid static and shaking cultures of *Ganoderma lucidum*. *Appl. Microbiol. Biotechnol.* **85**, 941–948 (2010).
14. Zhang, J. M., Zhong, J. J. & Geng, A. L. Improvement of ganoderic acid production by fermentation of *Ganoderma lucidum* with cellulase as an elicitor. *Process. Biochem.* **49**, 1580–1586 (2014).
15. Ren, A. et al. Methyl jasmonate induces ganoderic acid biosynthesis in the basidiomycetous fungus *Ganoderma lucidum*. *Bioresour. Technol.* **101**, 6785–6790 (2010).
16. Zhang, D. H. et al. Overexpression of the squalene epoxidase gene alone and in combination with the 3-hydroxy-3-methylglutaryl coenzyme a gene increases ganoderic acid production in *Ganoderma lingzhi*. *J. Agric. Food Chem.* **65**, 4683–4690 (2017).
17. Yuan, W. et al. Biosynthesis of mushroom-derived type II ganoderic acids by engineered yeast. *Nat. Commun.* **13**, 7740 (2022).
18. Liu, R. et al. SA inhibits complex III activity to generate reactive oxygen species and thereby induces GA overproduction in *Ganoderma lucidum*. *Redox Biol.* **16**, 388–400 (2018).
19. Zhang, X. et al. Heat stress modulates mycelium growth, heat shock protein expression, ganoderic acid biosynthesis, and hyphal branching of via cytosolic Ca^{2+}. *Appl. Environ. Microbiol.* **82**, 4112–4125 (2016).
20. You, B. J. et al. Induction of apoptosis and ganoderic acid biosynthesis by cAMP signaling in. *Sci. Rep.* **7**, 318 (2017).
21. Liu, Y. N. et al. Phospholipase D and phosphatidic acid mediate heat stress induced secondary metabolism in Ganoderma lucidum. *Environ. Microbiol.* **19**, 4657–4669 (2017).
22. Liu, Y. N. et al. Conversion of phosphatidylinositol (PI) to PI4-phosphate (PI4P) and then to PI(4,5)P_2 is essential for the cytosolic Ca^{2+} concentration under heat tress in. *Environ. Microbiol.* **20**, 2456–2468 (2018).

23. Pokotylo, I., Kravets, V., Martinec, J. & Ruelland, E. The phosphatidic acid paradox: too many actions for one molecule class? Lessons from plants. *Prog. Lipid Res.* **71**, 43–53 (2018).
24. Tanguy, E., Wang, Q. L., Moine, H. & Vitale, N. Phosphatidic acid: from pleiotropic functions to neuronal pathology. *Front. Cell Neurosci.* **13**, 2 (2019).
25. Fang, Y., Vilella-Bach, M., Bachmann, R., Flanigan, A. & Chen, J. Phosphatidic acid-mediated mitogenic activation of mTOR signaling. *Science* **294**, 1942–1945 (2001).
26. Dogliotti, G. et al. Membrane-binding and activation of LKB1 by phosphatidic acid is essential for development and tumour suppression. *Nat. Commun.* **8**, 15747 (2017).
27. Jang, J. H., Lee, C. S., Hwang, D. & Ryu, S. H. Understanding of the roles of phospholipase D and phosphatidic acid through their binding partners. *Prog. Lipid Res.* **51**, 71–81 (2012).
28. Testerink, C., Larsen, P. B., van der Does, D., van Himbergen, J. A. & Munnik, T. Phosphatidic acid binds to and inhibits the activity of Arabidopsis CTR1. *J. Exp. Bot.* **58**, 3905–3914 (2007).
29. Xie, L. J. et al. Unsaturation of very-long-chain ceramides protects plant from hypoxia-induced damages by modulating ethylene signaling in Arabidopsis. *PLoS Genet* **11**, e1005143 (2015).
30. Yao, H. Y., Wang, G. L., Guo, L. & Wang, X. M. Phosphatidic acid interacts with a MYB transcription factor and regulates its nuclear localization and function in Arabidopsis. *Plant Cell* **25**, 5030–5042 (2013).
31. Kim, S. C., Nusinow, D. A., Sorkin, M. L., Pruneda-Paz, J. & Wang, X. M. Interaction and regulation between lipid mediator phosphatidic acid and circadian clock regulators. *Plant Cell* **31**, 399–416 (2019).
32. Liu, Y.-N. et al. The bHLH-zip transcription factor SREBP regulates triterpenoid and lipid metabolisms in the medicinal fungus *Ganoderma lingzhi*. *Commun. Biol.* **6**, 1 (2023).
33. Yip, C. K., Murata, K., Walz, T., Sabatini, D. M. & Kang, S. A. Structure of the human mTOR complex I and its implications for rapamycin inhibition. *Mol. Cell.* **38**, 768–774 (2010).
34. David et al. RAFT1: A mammalian protein that binds to FKBP12 in a rapamycin-dependent fashion and is homologous to yeast TORs. *Cell* **78**, 35–43 (1994).
35. Mishkind, M., Vermeer, J. E. M., Darwish, E. & Munnik, T. Heat stress activates phospholipase D and triggers PIP_2 accumulation at the plasma membrane and nucleus. *Plant J.* **60**, 10–21 (2009).
36. Zhang, Y. Y. et al. Phospholipase D alpha 1 and phosphatidic acid regulate nadph oxidase activity and production of reactive oxygen species in ABA-mediated stomatal closure in Arabidopsis. *Plant Cell* **21**, 2357–2377 (2009).
37. DeBose-Boyd, R. A. et al. Transport-dependent proteolysis of SREBP: relocation of site-1 protease from Golgi to ER obviates the need for SREBP transport to Golgi. *Cell* **99**, 703–712 (1999).
38. Quinn, W. J. & Birnbaum, M. J. Distinct mTORC1 pathways for transcription and cleavage of SREBP-1c. *Proc. Natl Acad. Sci. USA* **109**, 15974–15975 (2012).
39. Yecies, J. L. et al. Akt stimulates hepatic SREBP1c and lipogenesis through parallel mTORC1-dependent and independent pathways. *Cell Metab.* **14**, 21–32 (2011).
40. Kamisuki, S. et al. A small molecule that blocks fat synthesis by inhibiting the activation of SREBP. *Chem. Biol.* **16**, 882–892 (2009).
41. Yi, J. M., Zhu, J. J., Wu, J., Thompson, C. B. & Jiang, X. J. Oncogenic activation of PI3K-AKT-mTOR signaling suppresses ferroptosis via SREBP-mediated lipogenesis. *Proc. Natl Acad. Sci. USA* **117**, 31189–31197 (2020).
42. Kan, Y., Mu, X. R., Gao, J., Lin, H. X. & Lin, Y. The molecular basis of heat stress responses in plants. *Mol. Plant* **16**, 1612–1634 (2023).
43. Kerbler, S. M. & Wigge, P. A. Temperature sensing in plants. *Annu. Rev. Plant Biol.* **74**, 341–366 (2023).
44. Yoshihara, T. et al. Heat stress activates the Akt/mTOR signalling pathway in rat skeletal muscle. *Acta Physiol.* **207**, 416–426 (2013).
45. Takahara, T. & Maeda, T. Transient sequestration of TORC1 into stress granules during heat stress. *Mol. Cell* **47**, 242–252 (2012).
46. Zhang, G., Wang, Z., Du, Z. & Zhang, H. mTOR regulates phase separation of PGL granules to modulate their autophagic degradation. *Cell* **174**, 1492–1506.e1422 (2018).
47. Veverka, V. et al. Structural characterization of the interaction of mTOR with phosphatidic acid and a novel class of inhibitor: compelling evidence for a central role of the FRB domain in small molecule-mediated regulation of mTOR. *Oncogene* **27**, 585–595 (2008).
48. Rodriguez Camargo, D. C., Link, N. M. & Dames, S. A. The FKBP-rapamycin binding domain of human TOR undergoes strong conformational changes in the presence of membrane mimetics with and without the regulator phosphatidic acid. *Biochemistry* **51**, 4909–4921 (2012).
49. Foster, D. A. Phosphatidic acid and lipid-sensing by mTOR. *Trends Endocrinol. Metabol.* **24**, 272–278 (2013).
50. Frias, M. A. et al. Phosphatidic acid drives mTORC1 lysosomal translocation in the absence of amino acids. *J. Biol. Chem.* **295**, 263–274 (2020).
51. Toschi, A. et al. Regulation of mTORC1 and mTORC2 complex assembly by phosphatidic acid: competition with rapamycin. *Mol. Cell. Biol.* **29**, 1411–1420 (2009).
52. Chen, Y., Zheng, Y. & Foster, D. A. Phospholipase D confers rapamycin resistance in human breast cancer cells. *Oncogene* **22**, 3937–3942 (2003).
53. Espenshade, P. J. SREBPs: sterol-regulated transcription factors. *J. Cell Sci.* **119**, 973–976 (2006).
54. Peterson, T. R. et al. mTOR complex 1 regulates lipin 1 localization to control the SREBP pathway. *Cell* **146**, 408–420 (2011).
55. Owen, J. L. et al. Insulin stimulation of SREBP-1c processing in transgenic rat hepatocytes requires p70 S6-kinase. *Proc. Natl Acad. Sci. USA* **109**, 16184–16189 (2012).
56. Radhakrishnan, A., Goldstein, J. L., McDonald, J. G. & Brown, M. S. Switch-like control of SREBP-2 transport triggered by small changes in ER cholesterol: a delicate balance. *Cell Metab.* **8**, 512–521 (2008).
57. Rawson, R. B. The SREBP pathway-insights from Insigs and insects. *Nat. Rev. Mol. Cell Biol.* **4**, 631–640 (2003).
58. Kober, D. L. et al. Identification of a degradation signal at the carboxy terminus of SREBP2: a new role for this domain in cholesterol homeostasis. *Proc. Natl Acad. Sci. USA* **117**, 28080–28091 (2020).
59. Stewart, E. V. et al. Yeast SREBP cleavage activation requires the Golgi Dsc E3 ligase complex. *Mol. Cell* **42**, 160–171 (2011).
60. Willger, S. D. et al. Dsc orthologs are required for hypoxia adaptation, triazole drug responses, and fungal virulence in *Aspergillus fumigatus*. *Eukaryot. Cell* **11**, 1557–1567 (2012).
61. Robichon, C. & Dugail, I. De novo cholesterol synthesis at the crossroads of adaptive response to extracellular stress through SREBP. *Biochimie* **89**, 260–264 (2007).
62. Jungmichel, S. et al. Specificity and commonality of the phosphoinositide-binding proteome analyzed by quantitative mass spectrometry. *Cell Rep.* **6**, 578–591 (2014).
63. Ren, A. et al. Transcript and metabolite alterations increase ganoderic acid content in *Ganoderma lucidum* using acetic acid as an inducer. *Biotechnol. Lett.* **36**, 2529–2536 (2014).

Acknowledgements

This work was supported by grants from National Natural Science Foundation of China (31900027, 32071673 and 32471816), the China Postdoctoral Science Foundation (2020M682601), the Science and Technology Innovation Program of Hunan Province (2023RC3157 and 2021RC4063), the Natural Science Foundation of Hunan Province (2024JJ5629), the Scientific Research Fund of Hunan Provincial Education Department, China (No. 22A0188 and 23A0229), the Natural Science Foundation of Changsha (Science and Technology Plan Project of

Changsha, kq2402252), and the Hunan Provincial Innovation Foundation for Postgraduates(CX20240688).

Author contributions

Y.-N.L. designed the study. Y.-L.C., Z.-J.Z., F.-Y.W, H.-J. W and Y.-N.L. carried out experiments and analyzed data. Y.-N.L. wrote the manuscript. X.-L.W. performed data curation. G.-Q.L. contributed to overall supervision, reviewing and editing the manuscript. All authors gave input and approved the manuscript.

Competing interests

The authors declare no competing interests.

Additional information

Supplementary information The online version contains supplementary material available at https://doi.org/10.1038/s42003-024-07225-y.

Correspondence and requests for materials should be addressed to Yong-Nan Liu or Gao-Qiang Liu.

Peer review information *Communications Biology* thanks Jia-Xun Feng and the other, anonymous, reviewer(s) for their contribution to the peer review of this work. Primary Handling Editor: David Favero.